JOURNAL OF AGRICULTURAL AND FOOD CHEMISTRY

Article

Discovery of Potent Succinate-ubiquinone Oxidoreductase Inhibitors via Pharmacophore-linked Fragment Virtual Screening (PFVS) Approach

Li Xiong, Xiao-Lei Zhu, Hua-Wei Gao, Yu Fu, Sheng-Qua Hu, Li-Na Jiang, Wen-Chao Yang, and Guang-Fu Yang

J. Agric. Food Chem., **Just Accepted Manuscript** • DOI: 10.1021/acs.jafc.6b00325 • Publication Date (Web): 26 May 2016

Discovery of Potent Succinate-ubiquinone Oxidoreductase Inhibitors *via* Pharmacophore-linked Fragment Virtual Screening (PFVS) Approach

Li Xiong,[1] Xiao-Lei Zhu,[1*] Hua-Wei Gao,[1] Yu Fu,[1] Sheng-Quan Hu,[1] Li-Na Jiang,[1] Wen-Chao Yang,[1] Guang-Fu Yang[1,2*]

[1]*Key Laboratory of Pesticide & Chemical Biology of Ministry of Education, College of Chemistry, Central China Normal University, Wuhan 430079, P.R. China*

[2]*Collaborative Innovation Center of Chemical Science and Engineering, Tianjin 30071, P.R.China*

Correspondence:

Guang-Fu Yang, Ph.D. & Professor

College of Chemistry

Central China Normal University

Luoyu Road 152, Wuhan 430079

P. R. China

TEL: 86-27-67867800

FAX: 86-27-67867141

E-mail: gfyang@mail.ccnu.edu.cn

Abstract:

Succinate-ubiquinone oxidoreductase (SQR) is an attractive target for fungicide discovery. Herein we report the discovery of novel SQR inhibitors using pharmacophore-linked fragment virtual screening approach, a new drug design method developed in our laboratory. Among newly designed compounds, compound **9s** was identified as the most potent inhibitor with the K_i value of 34 nM against porcine SQR, displaying about 10-fold higher potency than the commercial control penthiopyrad. The further inhibitory kinetics studies revealed that compound **9s** is a non-competitive inhibitor with respect to the substrate cytochrome *c* and DCIP. Interestingly, compounds **8a**, **9h**, **9j**, and **9k** exhibited good *in vivo* preventive effects against *Rhizoctonia solani.* The results obtained from molecular modeling showed that the orientation of R^2 group displayed a significant effect on the binding with the protein.

Key Words: Succinate-ubiquinone oxidoreductase, complex II, pharmacophore-linked fragment virtual screening, molecular modeling, structure-based design

Introduction

Pesticides play a key role in the control of diseases in crops, a vital part of ensuring global food security. However, the unrestricted use of highly toxic pesticides over several decades has resulted in negative effects on the environment and poisoning of nontargeted species. To reduce the negative impacts of the pesticides, new compounds with high efficacy and selectivity against target species are desirable.[1-2] Among the known pesticides classes, fungicides targeting succinate-ubiquinone oxidoreductase (SQR, EC 1.3.5.1, also known as succinate dehydrogenase or complex II) can offer such solutions. SQR is an important membrane complex in the tricarboxylic acid cycle (Kreb cycle) that catalyzes the oxidation of succinate to fumarate in the mitochondrial matrix as succinate dehydrogenase. Succinate oxidation is coupled to the reduction of ubiquinone to ubiquinol at the mitochondrial inner membrane as one part of the electron transfer chain. Electrons are transferred from succinate to ubiquinone through the burried prosthetic groups flavin-adenine dinucleotid (FAD), [2Fe-2S], [4Fe-4S], [3Fe-3S] clusters and heme, which form an integral part of SQR.[3-7] Due to its critical roles in life processes,[8-13] SQR has been identified as a promising action target for agricultural fungicides. SQR-inhibiting fungicides have many advantages, such as broad-spectrum fungi control (including resistance to other fungicides), excellent crop selectivity, benign environmental effects, low application rate, and low toxicity.

Since the launch of carboxin as the first commercial SQR fungicide in 1966,[14] about 18 commercial SQR fungicides have been successfully developed, which could be

classified into eight categories: pyrazole-4-carboxamides, thiazole carboxamides, pyridine carboxamides, phenyl-oxo-ethyl thiophene amide, oxathiin carboxamides, pyridinyl-ethyl benzamides, furan carboxamides, and phenyl-benzamides.[15] Our enzyme inhibition kinetics results showed that these carboxamide fungicides should bind into the ubiquinone-binding site (Q-site) of SQR.[16] The acyl moiety of carboxamide fungicides formed van-der-Waals (VDW) interactions with residues C_R46, C_S42, B_I218, and B_P169 of Q-site, and the carbonyl oxygen atom of the carboxamide formed H-bonds with residues B_W173 and D_Y91. These key interactions are highly conserved among different carboxamide fungicides. On the contrary, the hydrophobic sub-pocket surrounded by residues, C_W35, C_I43, and C_I30, extending to the mouth of the Q-site, can accommodate structurally-diverse and bulky amine groups. Therefore, the acyl moiety and amide bond could be regarded as the pharmacophore of the carboxamide fungicides. Modification of the amine moiety should be an effective way to obtain new inhibitors with improved potency.[17-20]

Recently, fragment-based drug discovery (FBDD) has been rapidly developed as an effective method of hit identification. Although FBDD has several significant advantages, such as higher ligand efficiency (LE), higher hit rate and more opportunities of structure optimization, it also poses great challenges. First, FBDD often relies on sensitive biophysical methods to detect the binding of fragments. Secondly, FBDD can only screen fragments with excellent solubility due to their much weaker binding affinity. Furthermore, FBDD requires large amounts of purified protein (>10 mg), which are very difficult to

achieve in most cases, especially for membrane proteins. In order to overcome the low-throughput nature of FBDD and meet these challenges, we developed a new approach named pharmacophore-linked fragment virtual screening (PFVS).[21] Using this new approach, we successfully discovered a series of new picomolar-range Q_o site inhibitors of the cytochrome bc_1 complex, an important membrane protein for drug and fungicide discovery. As a continuation of our computational discovery of new inhibitors of membrane protein, we extended the PFVS method to the SQR system with the pyrazole-carboxamide moiety as pharmacophore and designed a series of new potent SQR inhibitors. Herein, we report the discovery and structural optimization of indole-containing pyrazole-carboxamides, one of the hits identified by PFVS method. Very fortunately, one nanomolar SQR inhibitor was successfully obtained, with significantly improved potency compared with the commercial product penthiopyrad. In addition, some compounds displayed good preventive effects *in vivo* against *Rhizoctonia solani* (*R.solani*).

Materials and Methods

Chemicals

Unless otherwise noted, all chemical reagents were commercially purchased and treated with standard methods before use. Solvents were dried in a routine way and redistilled. *Rhizoctonia solani, Botrytis cinerea, Pseudoperonospora cubensis, Sphaerotheca fuliginea* were provided through the courtesy of the Center for Bioassay, Zhejiang Chemical Industry Research Institute. ^{1}H NMR spectra were recorded on a Mercury-Plus 400/600

spectrometer in $CDCl_3$ or DMSO with TMS as the internal reference. Mass spectral data were obtained on a MocroMass platform by electrospray ionization (ESI-MS). Elementary analyses were performed on a Vario EL III elementary analysis instrument. Melting points were taken on a Buchi B-545 melting point apparatus and uncorrected. The starting materials 2-(2-nitrophenyl) hydrazin-1-ium chloride, ethyl 2-oxopropanoate, 3-(difluoromethyl)-1- methyl-1*H*-pyrazole-4-carboxylic acid were commercially available.

Computational protocol

Based on the modification and combination of AutoGrow[22] and the Amber 8.0[23-25] programs, the PFVS method was designed to discovered new type SQR inhibitor. Depicted in Figure 1 is the workflow of PFVS calculations.

Synthetic Chemistry

The preparation of ethyl 2-methyl-3-[2-(2-nitrophenyl)hydrazono]propanoate, ethyl-7-nitro-1*H*-indole-2-carboxylate, 7-nitro-1*H*-indole-2-carboxylic acid, 7-nitro-1*H*-indole, N-substituted-7-nitro-1*H*-indole, N-substituted-1*H*-indol-7-amine and the title compounds 8-9 were performed according to the reported methods.[26,27] The detailed procedure and the characterization data were supplied in the Supporting Information.

Enzymatic Kinetics [28-29]

The preparation of succinate-cytochrome *c* reductase (SCR, mixture of respiratory SQR

and complex III) from porcine heart was essentially as reported[29]. The enzymatic activities of SCR, SQR and complex III were analyzed in respective reaction mixtures as reported previously[30-31]. Kinetic analyses for the inhibition mechanism were performed as previously described[29].

Data analysis[32]

According to the measured substance's extinction coefficient, the change of absorbance was converted to product variation, then making linear fitting of time, the slope is the enzymatic reaction velocity. Compared with the control sample, the inhibition rates of inhibitors were calculated.

Fungicidal Activity Assay

The fungicidal activities of compounds against *R. solani, B. cinerea, P. cubensis,* and *S. fuliginea* were evaluated according to a previously published method[33]. The results are summarized in Table 4.

Results and Discussion

Hit identification through PFVS

It may need to be pointed out that the PVFS is picking a new starting point for optimization, getting away from the "local minimum" of the current scaffold which has already been optimized, and ideally picking a starting point that can be optimized further

than the current scaffold. [34-36]

The workflow of hit identification via PFVS method is shown in Figure 1. The first key step of PFVS method is to define the pharmacophore. According to our previous study on enzyme inhibition kinetics of ten commercial carboxamide-type fungicides, we carried out systematic computational simulations of the interaction between SQR and carboxamide-type inhibitors. The results indicated that the acyl moiety and carboxamide group have relative conserved binding conformation (Supporting information, Figure 1S), and made great contribution to the inhibitor binding. Therefore, we defined the pyrazole-4-carboxamide moiety as the pharmacophore, the structure of the pharmacophore-bound SQR was prepared based on the computationally simulated penthiopyrad-SQR binding mode. Then, a modified library of 1735 fragments derived from commercial pesticides was screened and each fragment was set to link with the nitrogen atom of the pharmacophore. After performing a three-step computational screening (see Figure 1), 8 hits with the most favorable binding free energies (Supporting information, Figure 2S) were identified. Considering the synthetic feasibility, six hits **(3**, **4**, **5**, **6**, **7**, and **8**) were finally selected for further syntheses and structural optimization.

These six hit compounds were successfully synthesized and characterized using ^{1}H NMR and MS spectral data. However, hits **4**, **6** and **7** were eventually abandoned due to their too low inhibition activity (IC_{50} > 100 μM) towards porcine SQR. Fortunately, the IC_{50} values against porcine SCR of compounds **3**, **5**, and **8a** were found to be 24.39 μM, 19.79 μM, and 51.87 μM, respectively. Although compound **3** showed high inhibition effect against

143 porcine SQR, it was also eventually abandoned because further optimization of compound
144 **3** did not result in significant improvement of the potency. Finally, compounds **5** and **8**a
145 were allowed to progress to hit-to-lead chemistry. In this work, we only focused on the
146 structural optimization of hit **8**, the structural optimization of hit **5** will be reported
147 elsewhere.
148
149 **Optimization of Compound 8**
150 It is known that most of the commercial pyrazole-4-carboxamide fungicides have a CHF_2
151 group on the R^1 position of pyrazole ring.[15] Previously, we have also found that the -CHF_2
152 compound displayed higher potency than the corresponding -CF_3 compound.[37] Therefore, it
153 is not surprising that compound **8a** was first synthesized with -CHF_2 group on the R^1
154 position (Table 1). The binding mode of compound **8a** with SQR was shown in Figure 3A,
155 conservatively forming hydrogen bonds with B_W173 and D_Y91. The pyrazole ring of **8a**
156 inserted into the *Q*-site and formed cation-π interaction with C_R46, while the indole ring
157 is located in the entrance of the *Q*-site and formed hydrophobic interaction with C_I43,
158 similar to the binding mode of carboxin in 2WQY. The IC_{50} value of **8a** was 51.87 μM
159 against porcine SCR, still showing lower activity than the commercial control penthiopyrad
160 (IC_{50} = 1.32 μM). As we noted, the value of ΔE_{vdw} energy of **8a** was -39.60 kcal/mol, also
161 less favorable than that of penthiopyrad (ΔE_{vdw} = -41.91 kcal/mol, Table 2). Considering
162 the characteristic of *Q*-site, optimizing the hydrophobic interactions between the indole
163 ring and some important residues while keeping the key hydrogen bonds should be an

effective way to improve the potency. Bearing this consideration in mind, the -CH_3 or -CH_2CH_3 group was respectively introduced to result in **8b** and **8**c (Table 1). However, these two compounds almost showed no inhibition activity against porcine SCR (IC_{50} > 100μM). When introducing group -$CH_2CH_2CH_3$, the resulted compound **8d** (IC_{50} = 60.59μM) displayed the same level of activity as compound **8a**. When introducing -$CH_2CH_2CH_2CH_3$ group, the resulted compound **8e** (IC_{50} = 4.02 μM) showed about 13-fold improved potency than **8a**. As shown in Figure 3B, the -$CH_2CH_2CH_2CH_3$ group stayed nearly the same plane as the indole ring and its hydrophobic interaction with C_I43 and C_I30 was significantly improved. However, when introducing cyclopropylmethyl (**8**f), isobutyl (**8**g), cyclopentyl (**8**h), allyl (**8**i), prop-2-yn-1-yl (**8**j), the resulting compounds displayed lower activity, even complete loss of activity.

These results led us to carefully analyze the interaction between **8** and the protein. As shown in Table 2, the value of ΔE_{vdw} became more favorable with increasing the size of R^2 group, such as -39.60 kcal/mol for **8a** (R^2 = H), -41.43 kcal/mol for **8d** (R^2 = -CH_3), -44.28 kcal/mol for **8e** (R^2 = -$CH_2CH_2CH_2CH_3$). These results indicated that the substitute in R^2 position did increase the hydrophobic interaction between ligand and protein. However, compounds **8b-c** and **8f-h** displayed no inhibition towards porcine SCR, indicating that too small or too large group in R^2 position was unsuitable for the binding. In addition, when R^2 group changed from saturated alkyl to unsaturated alkyl, although the ΔE_{ele} energies contribution were increased, the less favorable entropy contributions (-$T\Delta$S) and polar solvation energies (ΔG_{pol}) were produced (e.g **8i** and **8j**), which accounted reasonably for

the lower activity of compounds **8f-j**.

Then, we attempted to introduce groups to the R^2 position linked directly with the N atom of the indole ring with the aim to increase the VDW interaction with some key residues. As we know, the entrance of the Q-site has some hydrophobic residues, such as D_Y91, C_W35, C_I43, and C_I30. How to modulate the conformation of indole ring to increase the VDW interaction with these residues was our primary concern. It has been well established that the aryl-aryl interaction energy is stronger than alkyl-aryl.[38] So, we introduced a hydrophobic benzyl group to link with the N atom of the indole ring, producing compound **9a** with just slightly increased activity (IC_{50} = 1.89 μM) as indicated by 8a. As shown in Figure 3C, the indole ring of **9a** took about 180° turn, and then resulted in the benzyl group forming edge-to-edge π-π interaction with D_Y91. As a result, the ΔE_{vdw} energy was increased to -46.35 kcal/mol. These results confirmed the reasonability of our hypothesis, and promoted us to design more compounds along with the same strategy.

In order to probe the structure-activity relationship of benzyl substitute, a number of benzyl substituted indoles containing pyrazole-carboxamide with diverse properties were synthesized (Table 1). A series of simple *para*-substituted benzyl groups such as 4-F (**9d**, IC_{50} = 0.44 μM), 4-Cl (**9g**, IC_{50} = 0.75 μM), 4-Br (**9i**, IC_{50} = 0.58 μM), and 4-OCH_3 (**9o**, IC_{50} = 0.80 μM) did produce a significant increase in activity over **9a**, but 4-CF_3 (**9l**, IC_{50} > 100 μM) and 4-OCF_3 (**9n**, IC_{50} > 100 μM) almost complete loss of activity. Meanwhile, *ortho*-substituted benzyl groups resulted in less or almost no activity, such as **9j** (2-CH_3,

206 IC_{50} = 8.45 μM), 2-F (**9b**, IC_{50} = 22.06 μM), 2-Cl (**9e**, IC_{50} > 100 μM), and 2-Br (**9h**, IC_{50} >
207 100 μM). For the derivatives bearing *meta*-substituted benzyl groups, compound **9c** (3-F,
208 IC_{50} = 2.76 μM) and **9m** (3-OCH_3, IC_{50} = 9.89 μM) showed a little decreased potency,
209 whereas **9f** (3-Cl, IC_{50} = 0.45 μM) and **9k** (3-CH_3, IC_{50} = 0.50 μM) showed about 4-fold
210 improved potency compared with **9a**. Interestingly, when introducing di-substituted benzyl
211 groups onto the N atom of the indole ring, the opposite results were obtained. As shown in
212 Table 1, **9q** (2,4-dichlorobenzyl, IC_{50} > 100 μM) exhibited almost no inhibition effects
213 towards porcine SCR, and **9r** (3,4-dimethylbenzyl, IC_{50} = 0.49 μM) exhibited strong
214 inhibition effects, but **9s** (3,5-dimethylbenzyl, IC_{50} = 0.09 μM) exhibited significant
215 inhibition effects with a IC_{50} of 0.09 μM, about 576-fold and 15-fold improvement,
216 respectively, over compound **8a** and the commercial control penthiopyrad (IC_{50} = 1.32 μM).
217 In Figure 3D, the carbonyl oxygen atom of **9s** formed hydrogen bonds with B_W173 and
218 D_Y91, the indole ring formed a cation-π interaction with C_R46, and the benzyl ring
219 formed an edge-to-edge π-π interaction with D_Y91. As a result, compound **9s** harvested
220 the largest ΔE_{vdw} and ΔG_{cal} energy with values of -51.08 kcal/mol and -17.38 kcal/mol,
221 respectively.

222 From the energy component analysis, we found that **9** analogues displayed relative larger
223 ΔE_{vdw} energy than **8** analogues. These results indicated that the hydrophobic interaction
224 between aryl-aryl were indeed stronger than alkyl-aryl. As shown in Table 2, both of the
225 electron-donating and electron-withdrawing groups attached on the benzyl always
226 increased the hydrophobic interaction. For example, the ΔE_{vdw} energies were -47.24

kcal/mol for **9b** (R^2 = 2-F), -48.86 kcal/mol for **9k** (R^2 = 3-CH_3), and -51.06 kcal/mol for **9m** (R^2 = 3-OCH_3).

To further understand the mechanism of inhibition of newly designed compounds, the binding mode of these compounds was superimposed. As shown in Figure 4, analogous to our previously study,[16] the pyrazol ring of the title compounds deeply inserted into the *Q*-site. The extremely interesting thing was that two directions were found when different substituted groups linked to indole ring. As for **8** derivatives, the alkyl group would mainly point to the left side from the perspective of Figure 4. On the contrary, the benzyl group in **9** derivatives primarily pointed to the right side, forming π-π interaction with D_Y91 (Figure 3C and 3D), perhaps correlating with higher activity compared to 8 derivatives. For example, compound **9k** (R^2 = 3-CH_3, IC_{50} = 0.50 μM) showed higher potency than **8b** (R^2 = -CH_3, IC_{50} >100 μM). It should be noted that the optimization of compound **8** was based on the above-mentioned computational strategy. The experimental and calculated binding free energies (ΔG) of compounds summarized in Table 2 showed a good linear correlation with the correlation coefficient of R^2 = 0.92, further confirming the reliability of this computational strategy (Supporting Information Figure 3S).

Inhibitory Kinetics of 9s and penthipyrad

In order to understand the mechanism by which these compounds inhibit this electron transport complex, compound **9s** was selected as an example to carry out further inhibitory kinetics against porcine SCR and SQR. As shown in Figure 5A, double-reciprocal plots

revealed the non-competitive inhibition of **9s** with respect to cytochrome *c*. Furthermore, we examined the effect of **9s** on the reactions of the SCR pathway catalyzed by SQR. We determined the kinetics of SQR activity with respect to the substrate DCIP in the absence and presence of **9s**. As shown in Figure 5B, **9s** was a non-competitive inhibitor against SQR with respect to the substrate DCIP. These results indicate that **9s** should bind to the *Q*-site of SQR, which is consistent with our previous study.[21] The commercial fungicide penthiopyrad also showed nearly the same chracteristics, non-competitive with respect to both cytochrome *c* and DCIP.[37]

Next, we compared the inhibitory activities of both compounds against porcine SCR and SQR (Table 3 and Figure 5). As indicated by the K_i values, Compound **9s** and penthiopyrad exhibited about 1.44-fold and 4.25-fold higher inhibition against the porcine SQR than SCR, respectively. We also found that compound **9s** and penthiopyrad nearly did not show any inhibitory effects against complex III at the concentration of 20μM (data not show). Furthermore, we also measured the IC_{50} values (Table 3) of **9s** and penthiopyrad against porcine SQR, showing about 2.3-fold and 2.5-fold more potent than against porcine SCR (Supporting Information Figure 4S). All these results indicated that the portion of complex III in SCR system did not display any effect upon the SQR assay. In addition, **9s** showed the same action mechanism as the commercial fungicide. Therefore, we can conclude that compound **9s** (K_i = 0.034 μM against porcine SQR) was indeed a potent SQR inhibitor, displaying about 10-fold higher potency than penthiopyrad (K_i = 0.33 μM).

***In vivo* test**

The antifungal activities of all of the titled compounds were evaluated against *R. solani*, *B. cinerea*, *P. cubensis*, and *S. fuliginea* in the greenhouse environment. Thifluzamide was used as the positive control, and the results were shown in Table 4. Thifluzamide did not exhibit fungicidal activity against *B. cinerea* and *P. cubensis* at a concentration of 100 mg/L, although it exhibited a total inhibition effect against *R.solani* and *S. filiginea*. As shown in Table 4, although showing lower fungicidal activity against *R.solani* and *S. filiginea* than Thifluzamide, some compounds still displayed inhibition effects to some extent against *R. solani* (**9i**: 54%, **9h**: 72%; **9k**: 73%, **9j**: 62%) and *S. filiginea* (**9n**: 60% and **9l**: 50%). In addition, all compounds along with the control thifluzamide displayed no inhibition against *B. cinerea* and *P. cubensis*. One of the possible reason of low *in vivo* activity of the newly designed compounds was due to the high reactivity of 3-position of indole ring, which resulted in the rapid metabolization of the title compounds in the plant. Researche has established that the indole derivatives were easily metabolized in wheat, pea, and rat liver tissues.[39-40] Therefore, all these results indicate that indole-containing pyrazole-carboxamide could be regarded as a new type of SQR inhibitor and further structural optimization should be carried out in the future.

Chemistry

The Figure 2 gives the steps necessary to synthesize **8a-j** and **9a-s** based on nucleophilic substitution reaction. N-substituted indol-7-amine was prepared by a multiple

step synthetic route using 2-(2-nitrophenyl)-hydrazin-1-ium chloride and 3-substituted-1-methyl-1*H*-pyrazole-4-carboxylic acid as starting materials. Finally, indol-7-amine reacted with 3-(difluoromethyl)-1-methyl-1*H*-pyrazole-4- carbonyl chloride to produce the title compound **8-9** smoothly. The synthesis routes for compound **4~7** was described in the Supporting information. The structure of all intermediates and designed compounds were confirmed by elemental analyses, by ^{1}H NMR and ESI-MS spectral data.

In summary, a series of novel indole-containing pyrazole-carboxamides **8-9** were rationally designed and synthesized based on the PFVS method. Among these compounds, compound **9s**, 3-(difluoromethyl)-*N*-[1-(3,5-dimethylbenzyl)-1*H*-indol-7-yl]-1-methyl-1*H*-pyrazole-4-carboxamide, displayed the most potent activity with the value of K_i 34 nM against porcine SQR. Further inhibitory kinetic assays indicated that compound **9s** was a non-competitive inhibitor with respect to the substrate cytochrome *c* and DCIP. The *in vivo* tests indicated that compounds **8a**, **9h**, **9j**, and **9k** exhibited well preventive effects against *R.solani* at the concentration of 100mg/L. The computational simulation results strongly indicated that the N-benzyl indole ring was favorable for the binding into the Q-site of SQR. The hydrogen bonds with D_Y91 and B_W173 and the cation-π interaction with C_R46 make great contribution to the binding free energy. In addition, the orientation of the group in R^2 position of the title compound has a significant effect on the potency.

SUPPORTING INFORMATION

Supplemental Figure 1S describes the chemical structure of ten commercial fungicides, Figure 2S shows the chemical structures of **8** top candidates, Figure 3S shows the coorelation between the calculated and experiment binding free energy, and Figure 4S describes the inhibition of **9s** against SCR and SQR, followed by the synthetic route of hit **3, 4**, **5**, **6, and 7**. These materials are available free of charge via the Internet at http://pubs.acs.org.

FUNDING

This research was supported by the Special Fund for Agro-scientific Research in the Public Interest (No. 201203022) and the National Natural Science Foundation of China (No. 21332004 and 21272092).

AUTHOR INFORMATION

Corresponding Author

*E-mail: (XLZ) xlzhu@mail.ccnu.edu.cn; (GFY) gfyang@mail.ccnu.edu.cn

NOTES

The authors declare no competing financial interest.

Reference:

1. Huang, J. X.; Jia, Y. M.; Liang, X. M.; Zhu, W, J.; Zhang, J. J.; Dong, Y. H.; Yuan, H. Z.; Qi, S. H.; Wu, J. P.; Chen, F. H.; Wang, D. Q. Synthesis and Fungicidal Activity of Macrolactams and Macrolactones with an Oxime Ether Side Chain. *J. Agric. Food Chem*. **2007**, *55*, 10857-10863.
2. Harsimran, K. G.; Harsh, G. Pesticides: Environmental Impacts and Management Strategies, Chapter 8, **2014**, 187-230.
3. Cecchini, G. Function and structure of complex II of the respiratory chain, *Annu. Rev. Biochem.* **2003**, *72*, 77-109.
4. Maklashina, E.; Cecchini, G. The quinone-binding and catalytic site of complex II, *Biochim. Biophys. Acta* **2010**, *1797*, 1877-1882.
5. Sun, F.; Huo, X.; Zhai, Y.; Wang, A.; Xu, J.; Su, D.; Bartlam, M.; Rao, Z. Crystal structure of mitochondrial respiratory membrane protein complex II, *Cell* **2005**, *121*, 1043-1057.
6. Yankovskaya, V.; Horsefield, R.; Tornroth, S.; Luna-Chavez, C.; Miyoshi, H.; Leger, C.; Byrne, B.; Cecchini, G.; Iwata, S. Architecture of Succinate Dehydrogenase and Reactive Oxygen Species Generation, *Science* **2003***, 299*, 700-704.
7. Hägerhäll, C. Succinate: quinone oxidoreductases, Variations on a conserved theme. *Biochim. Biophys. Acta* **1997**, *1320*, 107-141.
8. Ralph, S. J.; Moreno-Sánchez, R.; Neuzil, J.; Rodríguez-Enríquez, S. Inhibitors of Succinate: Quinone Reductase/Complex II Regulate Production of Mitochondrial Reactive Oxygen Species and Protect Normal Cells from Ischemic Damage but Induce Specific Cancer Cell Death, *Pharm. Res.* **2011**, *28*, 2695-2730.
9. Sierotzki, H.; Scalliet, G. A Review of Current Knowledge of Resistance Aspects for the Next-Generation Succinate Dehydrogenase Inhibitor Fungicides, *Phytopathology* **2013**, *103*, 880-887.
10. Harada, S.; Inaoka, D. K.; Ohmori, J.; Kita, K. Diversity of parasite complex II, *Biochim. Biophys. Acta* **2013**, *1827*, 658-667.

11. Huang, L. S.; Borders, T. M.; Shen, J. T.; Wang, C. J.; Berry, E. A. Crystallization of mitochondrial respiratory complex II from chicken heart: a membrane-protein complex diffracting to 2.0 Å, *Acta Cryst. Sect. D: Biol. Crystallogr* **2005**, *D61*, 380-387.
12. Huang, L. S.; Shen, J. T.; Wang, A. C.; Berry, E. A. Crystallographic studies of the binding of ligands to the dicarboxylate site of Complex II, and the identity of the ligand in the "oxaloacetate-inhibited" state, *Biochim. Biophys. Acta* **2006**, 1757, 1073-1083.
13. Huang, L. S.; Sun, G.; Cobessi, D.; Wang, A. C.; Shen, J. T.; Tung, E. Y.; Anderson, V. E.; Berry, E. A. 3-Nitropropionic Acid Is a Suicide Inhibitor of Mitochondrial Respiration That, upon Oxidation by Complex II, Forms a Covalent Adduct with a Catalytic Base Arginine in the Active Site of the Enzyme, *J. Biol. Chem*. **2006**, *281*, 5965-5972.
14. Gunasekaran, P.; Tauro, P. Mechanism of action of carboxin and the development of resistance in yeast, *J. Biosci*. **1982**, *4*, 219-225.
15. Mode of Action of Fungicides. FRAC Classification on Mode of Action, Crop life, 2015. http://www.frac.info.
16. Zhu, X. L.; Xiong, L.; Li, H.; Song, X. Y; Liu, J. J.; Yang, G. F. Computational and Experimental Insight into the Molecular Mechanism of Carboxamide Inhibitors of Succinate-ubquinone Oxidoreductase. *ChemMedChem* **2014**, *9*, 1512-1521.
17. Ye, Y. H.; Ma, L.; Dai, Z. C.; Xiao, Y.; Zhang, Y. Y.; Li, D. D.; Wang, J. X.; Zhu, H. L. Synthesis and Antifungal Activity of Nicotinamide Derivatives as Succinate Dehydrogenase Inhibitors, *J. Agric. Food Chem*. **2014**, *62*, 4063-4071.
18. Sun, J. S.; Zhou, Y. M. Synthesis and Antifungal Activity of the Derivatives of Novel Pyrazole Carboxamide and Isoxazolol Pyrazole Carboxylate, *Molecules*, **2015**, *20*, 4383-4394.

19. Wang, Z. J.; Gao, Y.; Hou, Y. L.; Zhang, C.; Yu, S. J.; Bian, Q.; Li, Z. M.; Zhao, W. G. Design, synthesis, and fungicidal evaluation of a series of novel 5-methyl-1H-1,2,3-trizole-4- carboxyl amide and ester analogues, *Eur. J. Med. Chem*. **2014**, *86*, 87-94.

20. Xiao, Y. S.; Yan, X. J.; Xu, Y. J.; Huang, J. X.; Yuan, H. Z.; Liang, X. M.; Zhang, J. J.; Wang, D. Q. Design, synthesis and fungiciddal activity of 11-alkoxyimino-5,6-dihydro-dibeno[b,e]azepine-6-one derivates, *Pest Manag. Sci*. **2013**, *69*, 814−826.

21. Hao, G. F.; Wang, F.; Li, H.; Zhu, X. L.; Yang, W. C.; Huang, L.S.; Wu, J.W.; Berry, E. A.; Yang, G. F. Computational discovery of picomolar Q(o) site inhibitors of cytochrome bc_1 complex, *J. Am. Chem. Soc.* **2012**, *134*, 11168-11176.

22. Durrant, J. D.; Amaro, R. E.; McCammon, J. A. AutoGrow: a novel algorithm for protein inhibitor design. *Chem. Biol. Drug Des*. **2009**, *73*, 168-178.

23. Hornak, V.; Abel, R.; Okur, A.; Strockbine, B.; Roitberg, A.; Simmerling, C. Comparison of multiple Amber force fields and development of improved protein backbone parameters, *Proteins* **2006**, *65*, 712-725.

24. Case, D. A. et al. AMBER 8; University of California: San Francisco, CA, **2004.**

25. Pan, Y. M.; Gao, D. Q.; Zhan, C. G. Modeling the catalysis of anti-cocaine catalytic antibody: competing reaction pathways and free energy barrier, *J. Am. Chem. Soc*. **2008**, *130*, 5140-5149.

26. Bie, J.; Liu, S.; Zhou, J.; Xu, B.; & Shen, Z. Design, synthesis and biological evaluation of 7-nitro-1H-indole-2-carboxylic acid derivatives as allosteric inhibitors of fructose-1,6-bisphosphatase. *Bioorg Med Chem*. **2014,** *22*, 1850-1862.

27. Chern, J. W.; Chen, G. S.; Chang, P. T.; Chen, K. Y.; Chen, M. L.; Lee, H. Y.; Chiou, C. T. **2012**, U.S. 8,173,693.

406 28. Zhao, P. L.; Wang, L.; Zhu, X. L.; Huang, X.; Zhan, C. G.; Wu, J. W.; Yang, G. F.
407 Subnanomolar inhibitor of cytochrome bc_1 complex designed by optimizing interaction
408 with conformationally flexible residues, *J. Am. Chem. Soc.* **2010**, *132*, 185-194.
409 29. King, T. E. Preparations of succinate-cytochrome *c* reductase and the cytochrome bc_1
410 particle, and reconstitution of succinate-cytochrome c reductase, *Methods Enzymol*.
411 **1967**, *10*, 216-225.
412 30. Fisher, N.; Bourges, I.; Hill, P.; Brasseur, G.; Meunier, B. Disruption of the interaction
413 between the Rieske iron-sulfur protein and cytochrome *b* in the yeast bc_1 complex
414 owing to a human disease-associated mutation within cytochrome *b*, *Eur. J. Biochem*.
415 **2004**, *271*, 1292-1298.
416 31. Fisher, N.; Brown, A. C.; Sexton, G.; Cook, A.; Windass, J.; Meunier, B. Modeling the
417 Q_o site of crop pathogens in *Saccharomyces cerevisiae* cytochrome *b*, *Eur. J. Biochem*.
418 **2004**, *271*, 2264-2271.
419 32. Wang, F.; Li, H.; Wang, L.; Yang, W. C.; Wu, J. W.; Yang, G. F. Design, syntheses, and
420 kinetic evaluation of 3-(phenylamino)oxazolidine-2,4-diones as potent cytochrome bc□
421 complex inhibitors, Bioorg. Med. Chem. 2011, 19, 4608-4615.
422 33. Huang, W.; Zhao, P. L.; Liu, C. L; Chen, Q.; Liu, Z. M.; Yang, G. F. Design, Synthesis,
423 and Fungicidal Activities of New Strobilurin Derivatives. *J. Agric. Food Chem.* **2007**,
424 *55*, 3004-3010.
425 34. Cui, H.; Kamal, Z.; Ai, T.; Xu, Y.; More, S. S.; Wilson, D. J.; Chen, L. Discovery of
426 potent and selective sirtuin 2 (SIRT2) inhibitors using a fragment-based approach, *J.*
427 *Med. Chem.* **2014**, *57*, 8340-8357.

35. Hajduk, P. J.; Greer, J. A decade of fragment-based drug design: Strategic advances and lessons learned, *Nat. Rev. Drug Discovery* **2007**, *6*, 211-219.

36. Rees, D. C.; Congreve, M.; Murray, C. W.; Carr, R. Fragment-based lead discovery. *Nat. Rev. Drug Discovery* **2004**, *3*, 660-672.

37. Xiong, L.; Zhu, X. L.; Shen, Y. Q.; Wickramabahu, KWMW.; Li, K.; Yang, G. F. Discovery of N-Benzoxazole-5-yl-Pyrazole-4-Carboxamide as Nanomolar SQR Inhibitors. *Eur. J. Med. Chem*. **2015**, *95*, 424-434.

38. Sanders, J. M. Optimal pi-stacking interaction energies in parallel-displaced aryl/aryl dimers are predicted by the dimer heavy atom count, *J. Phys. Chem. A*. **2010**, *114*, 9205-9211.

39. Chamberlain, K.; Wain, R. L. Studies on plant growth-regulating substances: The metabolism of indole-3-acetonitrile and related compounds in wheat and pea tissues, *Annals Applied Biology*, **1973**, *75*, 409-417.

40. King, L. J.; Parke, D. V.; Williams, R. T. The metabolism of [2-^{14}C]indole in the rat, *Biochem. J.* **1966**, *98*, 266-277.

FIGURE CAPTIONS

Figure 1. The protocl of PFVS.

Figure 2. General Synthesis of Compound **8-9.**

Figure 3. (A) The binding mode of **8a.** (B) The binding mode of **8e**. (C) The binding mode of **9a**. (D) The binding mode of **9s**.

Figure 4. The binding mode overlay of **8** (red stick) and **9** (blue stick) analogues in the Q-site of SQR.

Figure 5. Kinetic analysis of inhibition by **9s** (A for SCR and B for SQR) and penthiopyrad (C for SCR and D for SQR, obtained from ref 35) against porcine SCR and SQR. The inhibition of porcine SCR by (A) **9s** (1, 0 nM; 2, 10nM; 3, 30nM; 4, 50 nM and 5, 80 nM), (C) penthiopyrad (1, 0 nM; 2, 300nM; 3, 500 nM; 4, 1000 nM and 5, 2000 nM). Each reaction mixture contains 100 mM PBS (pH 7.4), 0.3 mM EDTA, 20 mM succinate, 0.1 nM enzyme, 1.16-16.0 μM cytochrome *c* and the indicated penthiopyrad or **9s**. K_i was estimated to be 0.049±0.002 μM for **9s** and 1.393±0.087 μM for penthiopyrad by assuming non-competitive inhibition. The inhibition of porcine SQR by (B) **9s** (1, 0 nM; 2, 5 nM; 3, 10 nM; 4, 30 nM and 5, 50 nM), (D)penthiopyrad (1, 0 nM; 2,100 nM; 3, 200 nM; 4, 300 nM and 5, 500 nM). Each reaction mixture contains 100 mM PBS (pH 7.4), 0.3 mM EDTA, 20 mM succinate, 2nM SCR, 1.18-41.22 μM DCIP and the indicated amount of penthiopyrad or **9s**. K_i was estimated to be 0.034±0.002 μM for **9s** and 0.327±0.009 μM for penthiopyrad by assuming non-competitive inhibition.

Table 1. Structures of compound **8-9** derivatives and their IC_{50} value against porcine SCR.

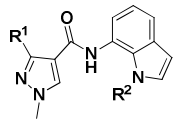

No.	R^1	R^2	IC_{50}（μM）	No.	R^1	R^2	IC_{50}（μM）
8a	CHF_2	H	51.87±1.22	**9**f	CHF_2	3-Cl-$PhCH_2$	0.45±0.01
8b	CHF_2	CH_3	>100	**9**g	CHF_2	4-Cl-$PhCH_2$	0.75±0.12
8c	CHF_2	CH_3CH_2	>100	**9**h	CHF_2	2-Br-$PhCH_2$	>100
8d	CHF_2	$CH_3CH_2CH_2$	60.59±3.46	**9**i	CHF_2	4-Br-$PhCH_2$	0.58±0.12
8e	CHF_2	$CH_3CH_2CH_2CH_2$	4.02±1.04	**9**j	CHF_2	2-CH_3-$PhCH_2$	8.45±1.14
8f	CHF_2	$(CH_2)_2CHCH_2$	>100	**9**k	CHF_2	3-CH_3-$PhCH_2$	0.50±0.13
8g	CHF_2	$(CH_3)_2CHCH_2$	>100	**9**l	CHF_2	4-CF_3-$PhCH_2$	>100
8h	CHF_2	$(CH_2)_5CH$	>100	**9**m	CHF_2	3-OCH_3-$PhCH_2$	9.89±1.07
8i	CHF_2	CH_2=$CHCH_2$	74.49±4.34	**9**n	CHF_2	4-OCF_3-$PhCH_2$	>100
8j	CHF_2	CH≡CCH_2	51.83±1.40	**9**o	CHF_2	4-OCH_3-$PhCH_2$	0.80±0.11
9a	CHF_2	$PhCH_2$	1.89±1.13	**9**p	CHF_2	2,4-F_2-$PhCH_2$	21.57±1.66
9b	CHF_2	2-F-$PhCH_2$	22.06±1.24	**9**q	CHF_2	2,4-Cl_2-$PhCH_2$	>100
9c	CHF_2	3-F-$PhCH_2$	2.76±1.15	**9**r	CHF_2	3,4-$(CH_3)_2$-$PhCH_2$	0.49±0.13
9d	CHF_2	4-F-$PhCH_2$	0.44±0.07	**9**s	CHF_2	3,5-$(CH_3)_2$-$PhCH_2$	0.09±0.01
9e	CHF_2	2-Cl-$PhCH_2$	>100	Penthiopyrad			1.32±0.11

Table 2. The individual energy terms of the calculated free energy of title compounds (kcal/mol).

No.	ΔE_{ele}	ΔE_{vdw}	ΔG_{np}	ΔG_{pol}	ΔH	$-T\Delta S$	ΔG_{cal}	ΔG_{exp} [a]
8a	-23.33	-39.60	-4.47	46.95	-20.46	10.16	-10.30	-5.82
8d	-18.48	-41.43	-4.86	44.42	-20.36	10.40	-9.96	-5.73
8e	-14.66	-44.28	-5.39	42.29	-22.04	10.05	-11.99	-7.33
8i	-20.38	-42.8	-4.84	47.31	-20.05	11.58	-8.47	-5.61
8j	-21.33	-41.99	-4.91	45.88	-22.35	11.74	-10.61	-5.82
9a	-25.54	-46.35	-5.25	53.48	-23.66	11.71	-11.95	-7.78
9b	-18.89	-47.24	-5.34	46.97	-24.50	8.25	-11.25	-6.33
9c	-20.36	-47.70	-5.37	50.84	-22.60	10.22	-12.38	-7.55
9d	-21.33	-47.50	-5.25	48.10	-25.98	10.23	-15.75	-8.64
9f	-25.24	-48.44	-5.41	52.62	-26.47	10.85	-15.62	-8.63
9g	-21.15	-48.39	-5.29	50.33	-24.50	10.01	-14.49	-8.32
9i	-19.35	-48.93	-5.48	50.01	-23.76	8.41	-15.35	-8.48
9j	-24.8	-47.43	-5.41	53.80	-23.16	10.82	-12.34	-6.89
9k	-22.14	-48.86	-5.40	51.28	-25.11	9.94	-15.17	-8.56
9m	-25.79	-51.06	-5.52	57.60	-24.77	12.74	-12.03	-6.80
9o	-29.85	-46.73	-5.36	56.22	-25.72	11.25	-14.47	-8.29
9p	-19.53	-46.15	-5.36	48.17	-22.87	11.45	-11.42	-6.34
9r	-16.24	-45.70	-5.37	42.12	-25.19	9.55	-15.64	-8.57
9s	-23.14	-51.08	-5.61	52.18	-27.66	10.28	-17.38	-9.59
Penthiopyrad	-13.84	-41.91	-5.10	34.28	-26.57	13.54	-13.03	-7.99

[a] $\Delta G_{exp} = -RTLnIC_{50}$

Table 3. The inhibitory effect of some inhibitors against porcine SCR and SQR.

Inhibitor	SCR (succinate-cyt.*c* system 23°C)			SQR (DCIP-system 23°C)		
	IC_{50} (μM)	Inhibition type (with cyt. *c*)	K_i (μM)	IC_{50} (μM)	Inhibition type (with DCIP)	K_i (μM)
9s	0.090±0.01	non-competitive	0.049±0.002	0.040±0.004	non-competitive	0.034±0.002
penthiopyrad[a]	1.32±0.110	non-competitive	1.39±0.087	0.53±0.111	non-competitive	0.33±0.009

[a] The data were taken from ref 37.

Table 4. The titled compounds fungicidal activities *in vivo*.

No.	concentration (mg/L)	*R. solani*	*B.cinerea*	*P.cubensis*	*S. filiginea*
8a	100	68	0	0	20
8b	100	44	0	0	0
8c	100	0	0	0	0
8d	100	0	0	0	0
8e	100	31	0	0	0
8f	100	0	0	0	0
8g	100	0	0	0	0
8h	100	22	0	0	0
8i	100	0	0	0	0
8j	100	0	0	0	0
9a	100	0	0	0	0
9b	100	0	0	0	0
9c	100	0	0	0	0
9d	100	0	0	0	0
9e	100	0	0	0	0
9f	100	18	0	0	0
9g	100	18	0	0	0
9h	100	72	0	0	0
9i	100	54	0	0	0
9j	100	62	0	0	0
9k	100	73	0	0	0
9l	100	0	0	0	50
9m	100	0	0	0	0
9n	100	0	0	0	60
9o	100	0	0	0	0
9p	100	0	0	0	0
9q	100	11	0	0	0
9r	100	0	0	0	0
9s	100	0	0	0	0
Thifluzamide	100	100	0	0	100

Figure 1.

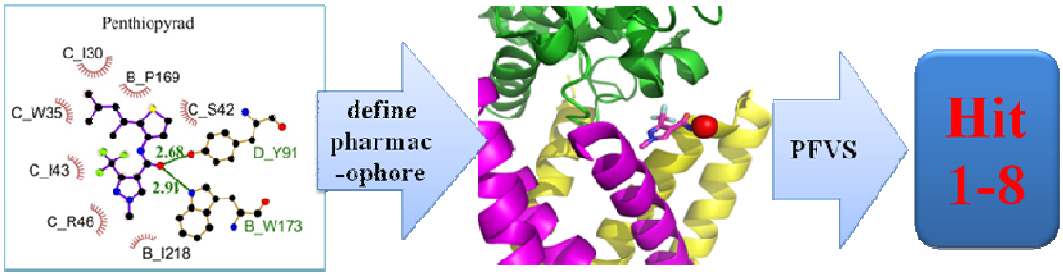

the binding mode of penthiopyrad

Figure 2.

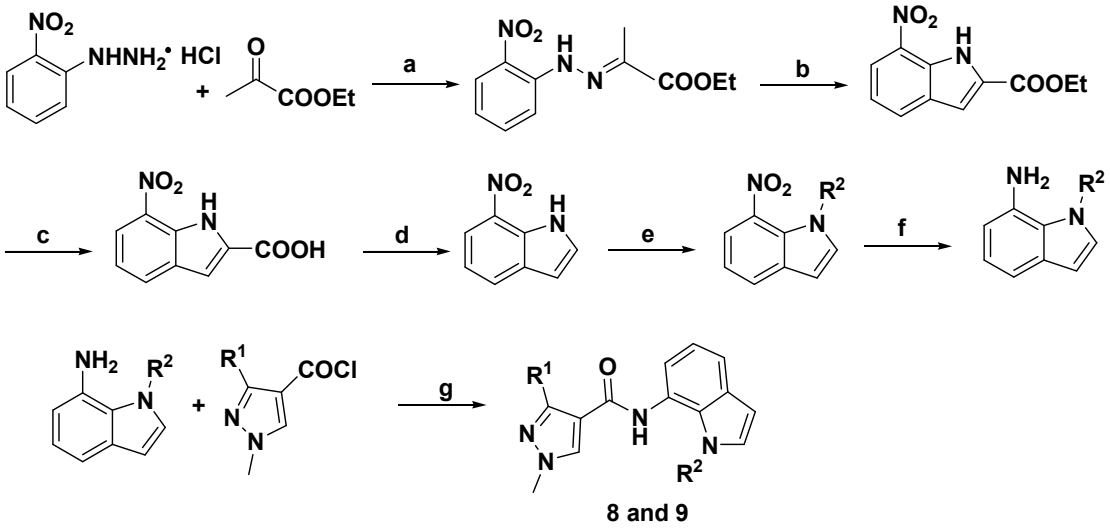

(a) NaOAc, MeOH, rt. (b) PPA,110 □ (c) NaOH/H_2O, 45 □ ; HCl, 40 □ (d) CuO, quinoline, 194 □ (e) NaH/DMF, R^2X (f) EtOH/H_2O, Fe, NH_4Cl, reflux (g) $(CH_3CH_2)_3N$, CH_2Cl_2, 0 □

Figure 3.

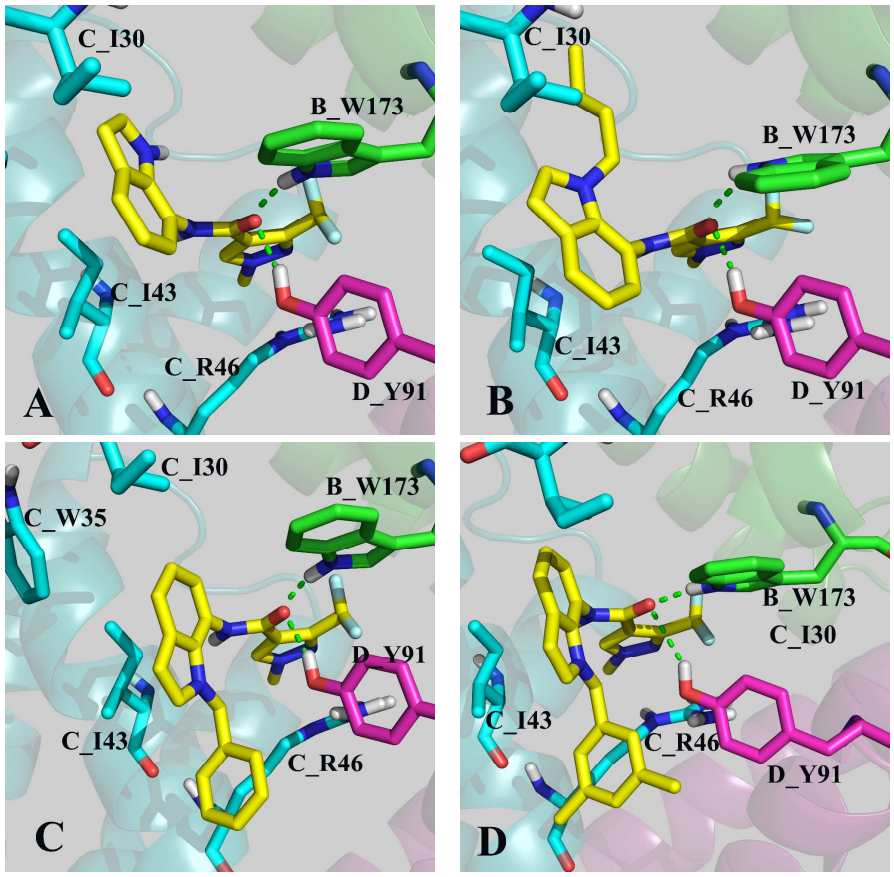
C_I30
B_W173
C_I43
C_R46
D_Y91
A
C_I30
B_W173
C_I43
C_R46
D_Y91
B
C_I30
B_W173
C_W35
D_Y91
C_I43
C_R46
C
B_W173
C_I30
C_I43
C_R46
D_Y91
D

Figure 4.

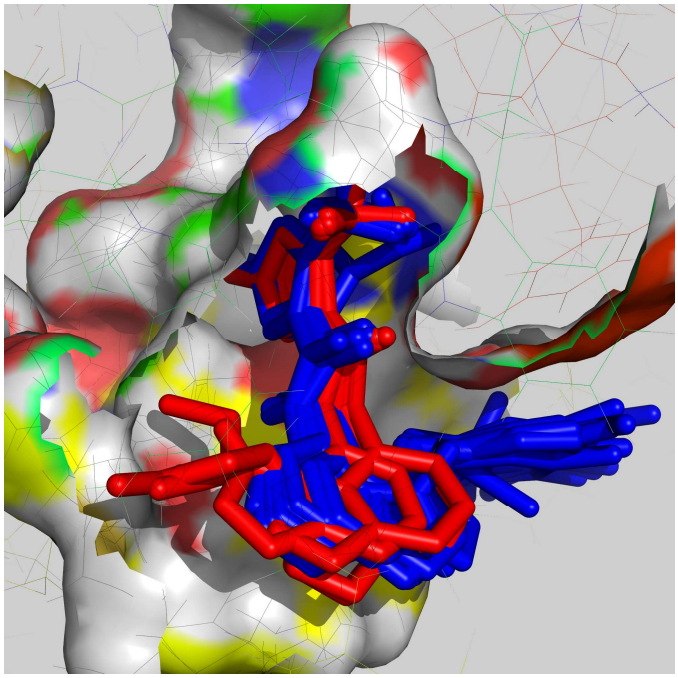

Figure 5.

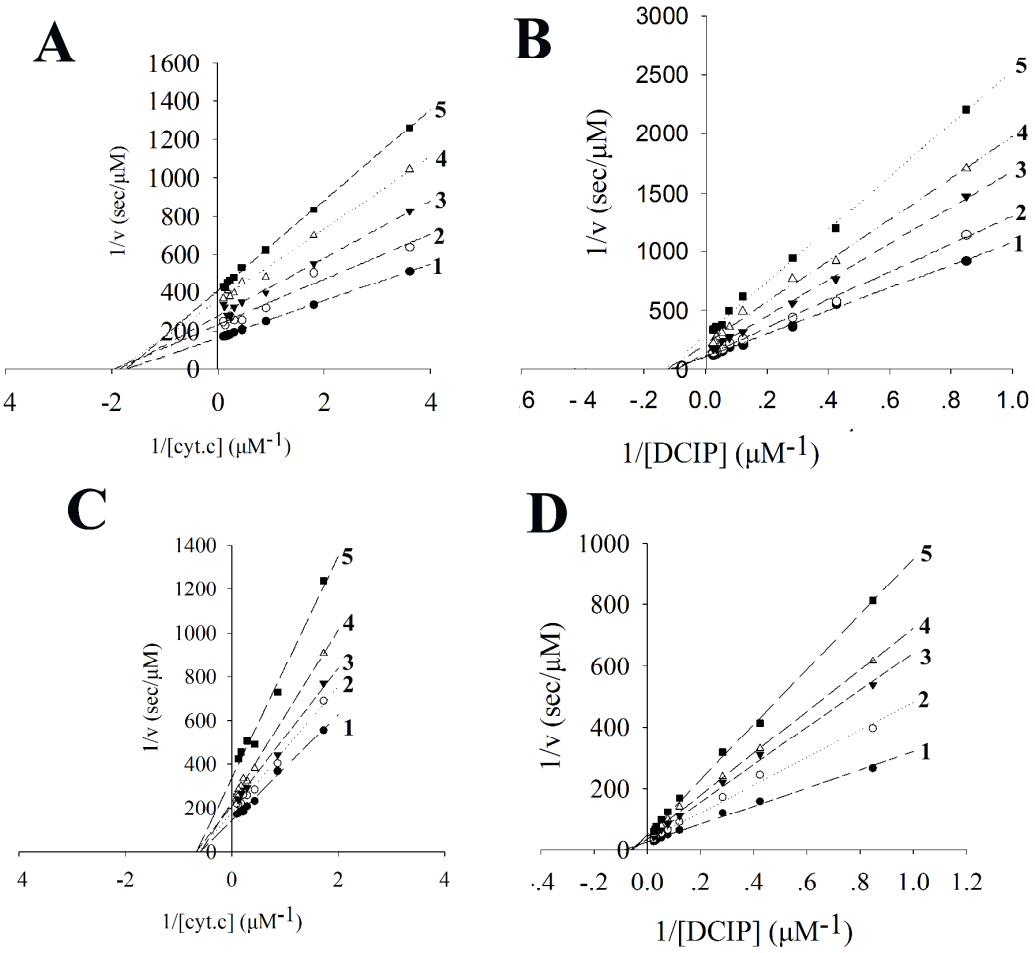
A
1600
1400
1200
1000
800
600
400
200
0
1/v (sec/μM)
5
4
3
2
1
4
-2
0
2
4
1/[cyt.c] (μM-1)
B
3000
2500
2000
1500
1000
500
0
1/v (sec/μM)
5
4
3
2
1
.6
- 4
-.2
0.0
.2
.4
.6
.8
1.0
1/[DCIP] (μM-1)
C
1400
1200
1000
800
600
400
200
0
1/v (sec/μM)
5
4
3
2
1
4
-2
0
2
4
1/[cyt.c] (μM-1)
D
1000
800
600
400
200
0
1/v (sec/μM)
5
4
3
2
1
.4
-.2
0.0
.2
.4
.6
.8
1.0
1.2
1/[DCIP] (μM-1)

TOC graphic